

ORIGINAL RESEARCH ARTICLE

Hydrothermal synthesis of valve metal Ta-doped titanate nanofibers for potentially engineering bone tissue

Parker Cole^{1,2,†}, Yang Tian^{2,3,†}, Savannah Thornburgh⁴, Mary Malloy⁴, Lauren Roeder⁴, Lu Zhang⁵, Mansi Patel⁶, Yiting Xiao⁷, Yan Huang⁸, Z. Ryan Tian^{2,3,5,6,*}

¹ Biomedical Engineering, University of Arkansas, Fayetteville, AR 72701, USA

² Institute for Nanoscience/Engineering, University of Arkansas, Fayetteville, AR 72701, USA

³ Materials Science/Engineering, University of Arkansas, Fayetteville, AR 72701, USA

⁴ Biological Sciences, University of Arkansas, Fayetteville, AR 72701, USA

⁵ Cell/Molecular Biology, University of Arkansas, Fayetteville, AR 72701, USA

⁶ Chemistry/Biochemistry, University of Arkansas, Fayetteville, AR 72701, USA

⁷ Biological/Agricultural Engineering, University of Arkansas, Fayetteville, AR 72701, USA

⁸ Animal Science, University of Arkansas, Fayetteville, AR 72701, USA

* Corresponding author: Z. Ryan Tian, rtian@uark.edu

† These authors contributed equally to this work.

ABSTRACT

Recent research efforts have increasingly concentrated on creating innovative biomaterials to improve bone tissue engineering techniques. Among these, hybrid nanomaterials stand out as a promising category of biomaterials. In this study, we present a straightforward, cost-efficient, and optimized hydrothermal synthesis method to produce high-purity Ta-doped potassium titanate nanofibers. Morphological characterizations revealed that Ta-doping maintained the native crystal structure of potassium titanate, highlighting its exciting potential in bone tissue engineering.

Keywords: nanosynthesis; titanate nanofiber; bone scaffold; tantalum dopant

ARTICLE INFO

Received: 12 December 2023

Accepted: 12 November 2023

Available online: 17 January 2024

COPYRIGHT

Copyright © 2024 by author(s).

Characterization and Application of Nanomaterials is published by EnPress Publisher LLC. This work is licensed under the Creative Commons Attribution-NonCommercial 4.0 International License (CC BY-NC 4.0).

<https://creativecommons.org/licenses/by-nc/4.0/>

1. Introduction

Recently, nanomaterials have garnered significant attention for their applications in bone tissue engineering due to their unique physicochemical properties. Implant materials can be enhanced by these artificially designed nanostructures to better mimic the native extracellular matrix, improve mechanical properties, support osteoconductive conditions, control drug delivery release, increase surface area and porosity, strengthen the cell-scaffold interaction, and even improve X-ray imaging quality^[1-9].

Since bone is a natural bio-nanocomposite, it has been our goal to develop functional nanoscale bone tissue substitutes that can be used to repair, replace, or regenerate damaged or diseased bone. Regarding recent studies on the impact of nanotechnology on orthopedic applications, the key factors at the nanoscale, including grain size, pore morphology, surface topography, surface area-to-volume ratio, surface wettability, and the corresponding energetics, have been identified as critical determinants for achieving superior performance^[8]. To this end, there has been a prolific surge in the exploration, development, and

implementation of diverse nanomaterials and associated nanocomposites within the field of bone tissue engineering^[9,10].

Titanium dioxide (TiO₂) has attracted significant attention in recent times, primarily due to the intersection of orthopedics and nanomaterial science. This surge in interest can be attributed to the well-established understanding that Ti metal undergoes surface oxidation when exposed to atmospheric conditions, culminating in the formation of a robust native TiO₂ layer on the external face. Techniques such as anodization further enhance this process, leading to the development of a passivated surface coating that is biologically compatible and osteogenic. Advancements in nanomaterial chemistry have been pivotal in this domain, enabling the controlled assembly of TiO₂ structures, including nanofibers and nanotubes. Furthermore, specific synthetic methods have been identified to produce titanate clusters that exhibit a layered structure, which is conducive to apatite formation—the inorganic composite of native bone tissue. It's also worth noting that titanium dioxide has the ability to react and transform into titanate nanotubes or nanowires. This characteristic has proven beneficial as it has been demonstrated to facilitate ion-exchange interactions with body fluids, thereby supporting bone tissue growth. Specifically, when titanate materials are placed in simulated body fluid, ionic exchange commences and encourages the generation of hydroxyapatite, a fundamental component of natural bone. Nanomaterials chemistry has enriched this area of research, and many labs have investigated structurally controlling TiO₂ morphologies such as nanofibers and nanotubes^[11,12]. Advancements in synthetic approaches have been identified to produce titanate materials, which are distinguished by their clay-like lattice, composed of edge-sharing TiO₆ octahedra interspersed with cationic entities^[13]. This stratified structure is particularly favorable for apatite formation in simulated body fluid (SBF). More specifically, the hydrothermal reaction involving powdery TiO₂ minerals, such as rutile and anatase, with aqueous sodium or potassium hydroxide solutions yields Na- or K-titanate nanotubes or nanowires, depending on reaction conditions. This resulting ionic-layered structure serves a crucial role as a cationic reservoir. It aids in ion-exchange with cations found in body fluids, thus autonomously maintaining cation equilibrium in situ, a process vital for bone tissue growth. In an SBF environment, the concentration gradient between Na/K-titanate and calcium (Ca²⁺) prompts the ion-exchange of monovalent Na⁺ or K⁺ ions with Ca²⁺. This sets the stage for a subsequent interaction: the coordination of phosphate anions {i.e., (PO₃)³⁻, (HPO₃)²⁻, and (H₂PO₃)⁻} from the body fluid with the titanate-bound Ca²⁺. The culmination of this interaction is the formation of hydrated calcium phosphate, or hydroxyapatite, an essential building block of natural bone^[13].

Tantalate-based nanomaterials have been demonstrated to be osteoconductive; however, their syntheses have not become commercially viable for large-scale production^[14-16]. In one instance, tantalum-coated polylactic acid (PLA) electrospun fibers were found to be more osteoconductive compared to bare PLA^[17]. Cell attachment, cell proliferation and preosteoblast differentiation were all improved in vitro^[17]. Congruently, Ta-PLA led to expedited bone tissue formation and provided a conducive environment for osteocytes to thrive in a rabbit calvarial defect model. Furthermore, an anodized layer of tantalum was added to a titanate nanotube-coated substrate and was shown to enhance the matrix mineralization rate by 30% compared to a control titanate-coated substrate^[14]. The doped titanate has provided an alternative strategy to hybridize other osteogenic elements (such as other valve metals: Zr, Nb, or Ta) into heterogenous nanostructures rather than try and develop difficult and/or costly approaches to obtain pure species such as Tantalum oxide and Tantalum pentoxide^[11,17-21]. Through this hydrothermal doping process, we strive to promote the integration of osteogenic elements without incurring risks associated with surface coating delamination (e.g., an inflammatory response to rogue metallic debris)^[17]. To evaluate new Ta-doped nanomaterials for bone tissue regeneration applications, we conducted a systematic nanosynthesis study to assess the feasibility of producing long and pristine nanofibers of Ta-doped titanate. Tantalum doping optimization was corroborated using

characterization data from scanning electronic microscopy with an energy-dispersive elemental analyzer (SEM-EDX) together with X-ray diffraction (XRD).

2. Materials and methods

2.1. Nanofiber synthesis

The Ta-doped potassium titanate nanofibers were prepared following a published protocol^[15,16,21,22] with some modifications. Briefly, in a Teflon cup containing 50 mL water solution of 10 M KOH, 500 mg of TiO₂ powder (Aeroxide P25) was added to the Teflon and stirred for about 5 min with a Teflon-coated magnetic stirring bar on an electrical stirrer. Thereafter, Tantalum pentoxide powder (chemical grade, from Johnson Matthey) was mixed with the KOH suspension for 24 h to form a mixture upon stirring. Here, the molar ratio of Ta-dopant to Ti was widely varied from 1%–4%.

Next, the mixture containing Teflon cup was sealed in an autoclave container, heated in an oven at 240 °C for 72 h and then allowed to cool to room temperature. The white powdery product was collected, water-washed until pH = 7, and finally air-dried for characterization. To keep the nanofiber lattice intact, it is important to do the water-washing step carefully, as detailed separately below.

2.2. Post synthesis washing

The fibers were formed as a slurry from the high alkalinity environment in the autoclave treatment. To remove the residual KOH, the white slurry went through a well-controlled neutralization process. The nanofiber slurry was first centrifuged for 5 min at 4000 rpm. The supernatant was decanted and then deionized water was mixed to form another slurry with a lower KOH content, which was repeated until the supernatant's pH = 7.

2.3. Characterization

The SEM-EDX analysis was carried out on the FEI Nova NanoLab 200 to assess nanofiber morphology and chemical composition. Typically, the fiber sample was placed on an aluminum holder to let the sample dry in air. Once dried, the holder was placed in a plasma sputtering coater with an Au target to coat the sample surface with Au. The XRD was performed with the Rigaku MiniFlex II Desktop X-ray diffractometer using monochromatized Cu-K α ($\lambda = 1.5406 \text{ \AA}$) at 30 kV and 15 mA, in the range of 2θ from 5° to 60° at a speed of 1°/min. to assess crystal structure.

3. Results and discussion

The Ta-doped potassium titanate nanofibers underwent self-assembly, forming a bone-mimetic bio-scaffold structure upon desiccation as illustrated in **Figure 1**. These self-assembled nanowires created micro-size porous structures, facilitating effective bone tissue adhesion to the bio-scaffold. Moreover, the increased surface area provided by these structures enhances osteoblast cell adhesion.

At higher magnification (**Figure 2(a)**) under the SEM, the well-crystallized long nanofibers in self-entangled sheets can be clearly seen, which is a characteristic of the successfully Ta-doped potassium titanate nanofibers. The nanofibers length extends into the microns range whereas their width is typically under 50 nm. Additionally, **Figure 2(a)** shows the relatively smooth surface of the high length to width ratio (or aspect ratio) nanofibers, suggesting an optimal control over the nanowires' nucleation and 1D-growth in nanoscale, which is crucial for the Mo-dopant's good distribution throughout the crystal lattice of all the nanowires from the "one-pot" nanosynthesis.

In the Energy-Dispersive X-ray (EDX) map, the Ta dopants (**Figure 2(d)**) and Ti (**Figure 2(c)**) are evenly distributed on the fibers. This uniformity in distribution suggests the dopant well-dispersed in the Ta-doped

titanate nanowires, which indicates a quite precisely controlled nano-synthesis process. Theoretically, the $[\text{TaO}_6]$ octahedron in the nanowire lattice is larger than the $[\text{TiO}_6]$ octahedra^[23]. However, the $[\text{TaO}_6]$ octahedra are well-dispersed allowing for the structural distortion of each $[\text{TaO}_6]$ octahedron to not disrupt the lattice structural continuity as suggested by the EDX mapping in **Figure 2**. In other words, the high dispersion of Ta dopant in the nanofiber structure suggests the optimal doping conditions that support **Figure 1**.

The nanofiber crystal structure can be characterized using the XRD patterns (**Figure 3**). All the XRD peaks of (200), (110), (310), $(31\bar{2})$, $(40\bar{4})$, and (020) can be assigned to the layered $\text{K}_2\text{Ti}_6\text{O}_{13}$ titanate lattice (JCPDS No. 40-0403). No residual impurity was detected, as evidenced by no extra peaks in the XRD pattern due to the XRD detection limit, which indicates that the larger $[\text{TaO}_6]$ octahedron is well-doped in the titanate crystal structure to maintain the lattice integrity and nanofiber structure.

Comparing the XRD pattern with against those without the doping (**Figure 4(a)**), the large Ta-dopant increases the d-space between adjacent titanate sheets by shifting the XRD peak to $d_{(200)} = 8.1215 \text{ \AA}$ (or a lower 2-theta angle at $2\theta = 10.89^\circ$) at 4% Ta-dopant. This is in contrast with the undoped nanofiber's smaller d-space of $d_{(200)} = 7.7415 \text{ \AA}$ at a higher 2-theta angle ($2\theta = 11.43^\circ$). This interlayer spacing expansion is indicative of Ta substitutional doping within the titanate lattice. More specifically, the ionic radius of Ta^{5+} (73 pm) is larger than that of Ti^{4+} (53 pm) which leads to Ta^{5+} species replacing Ti^{4+} within the titanate lattice^[23–25]. Substitutional doping of larger ions within the native lattice increases lattice parameters and cell volume resulting in shifts to lower diffraction angles^[16,24]. Moreover, the doped samples' XRD patterns show no structural impurity. This is because all the XRD peaks are in the same width and can be indexed to that of potassium titanate, matching what our lab reported in the literature before^[15,16].

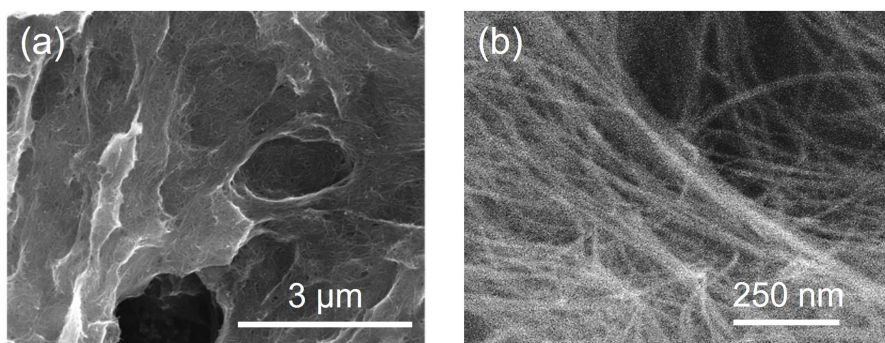


Figure 1. SEM micrographs of ta-doped potassium titanate.

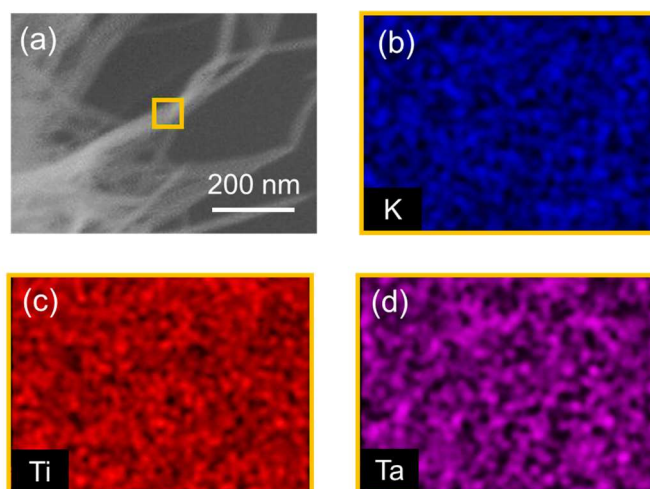


Figure 2. The EDX mapping of the Ta-doped potassium titanate nanofibers. (a) The high-resolution SEM of Ta-doped potassium with the yellow box for mapping. The EDX mapping showed that (b) K, (c) Ti, and (d) Ta are evenly distributed on the titanate nanofibers.

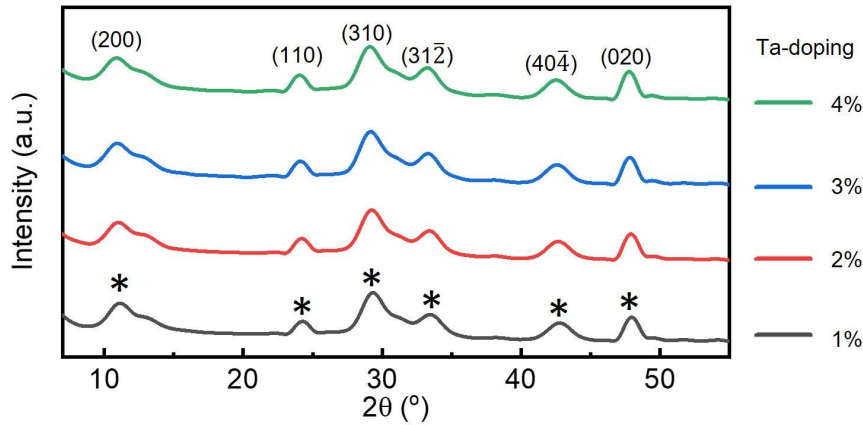


Figure 3. X-Ray diffraction of Nb-doped potassium titanate nanofibers with different doping percentages.

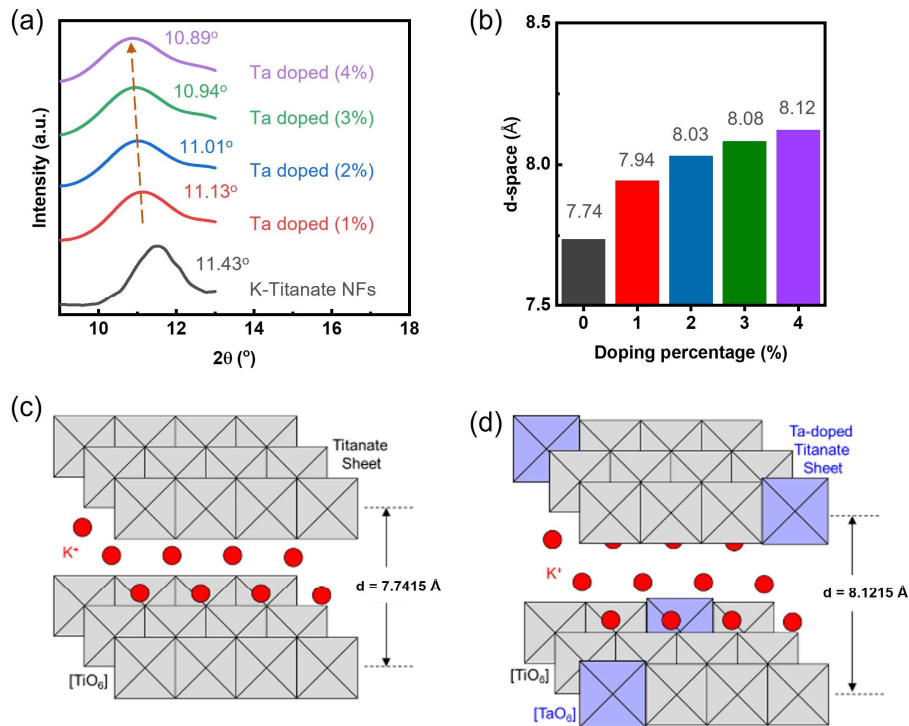


Figure 4. (a) XRD analysis of Ta-doped potassium titanate nanofibers with (b) d-space value. (c) and (d) schematics of Ta-dopant impact on the titanate crystal structure.

Within the clay-like layered crystal structure of K-titanate nanofibers, the Ti^{4+} -based $[\text{TiO}_6]$ octahedra were partially substituted with the Ta^{5+} -based $[\text{TaO}_6]$ octahedra by the deliberate doping of Ta. Sterically, the volumetrically larger $[\text{TaO}_6]$ octahedra, in comparison to $[\text{TiO}_6]$, would preferentially orient themselves on the nanofiber surface to minimize disruptions within the predominantly $[\text{TiO}_6]$ crystal lattice. Such surface-localized $[\text{TaO}_6]$ entities have been identified as promoters of bone-tissue adhesion, as supported by prior literature^[26,27]. Moreover, the adjacent interlayer K^+ cations in proximity to the $[\text{TaO}_6]$ within the K-titanate nanofiber are inclined to undergo rapid substitution by Ca^{2+} cations present in body fluids. This promotes the rapid nucleation of hydrated calcium phosphates, notably hydroxyapatite, on the nanofiber surface, aligning with observations made by other researchers in simulated body fluid (SBF) experiments^[13,28]. The strong affinity between the hydroxyapatite layer and the foundational titanate nanofiber ensures persistent bone tissue adhesion on the hydroxyapatite-coated nanofiber, establishing an ideal osteogenic and osteoconductive environment^[13]. As such, the enhanced surface properties of titanate nanofibers offer a synergistic strategy to current practices, augmenting the osteoconductivity of bone scaffolds^[26,29]. At its core, this study presents an

innovative and cost-effective method for integrating Ta (V) into the titanate nanofiber matrix, representing a notable advancement in orthopedic nanomedicine.

4. Conclusions

Tantalum-doped potassium titanate nanofibers have been satisfactorily synthesized through a straightforward hydrothermal method. To the best of our knowledge, this approach represents a novel contribution, particularly within the domain of orthopedic nanomedicine. The nanofibers retained their morphological, compositional, and crystalline attributes after doping, demonstrating the efficacy of the hydrothermal method in facilitating crystal framework doping. Furthermore, the dopant concentrations were carefully modulated to ensure no deleterious effects on the nanofiber's lattice structure, a pivotal consideration for preserving the nanofibers' intrinsic properties for their intended applications. To evaluate the impact of this material on bone tissue engineering, nanofibers with diverse Ta-dopant concentrations will be subjected to *in vitro* and *in vivo* protocols, aiming to gauge their biocompatibility and osteogenic capacity. Ultimately, the goal of this research is to identify the most effective Ta-doped titanate nanofiber composition to be used in biomaterial matrices to improve the osteogenic properties of bone cement.

Understanding the impact of biocompatible transition metal doping on the physicochemical properties of nanofiber-based bone implants is imperative for the design of biomaterials tailored to each distinct application. The interactions between these doped nanofibers and bone cells will garner critical insights into their prospective utility as candidates for bone tissue composites—a standard criterion in determining the appropriateness of materials for clinical applications.

A progressive strategy stemming from this research is the doping of titanate nanofibers with dual oxide dopants, potentially facilitating the investigation of a broadening spectrum of bone tissue composites characterized by diverse physiological adaptability.

This approach empowers researchers to systematically investigate the effects of doping variations on the material's properties and efficacy. The insights derived from such studies are crucial for the fine-tuning of these materials, optimizing them for targeted applications within bone tissue engineering and beyond.

Data availability statement

Applicable for reasonable request.

Author contributions

Investigation, PC, YT, ST, MM, LR, MP and YX; writing—original draft preparation, PC, YT and ZRT; writing—review and editing, PC, YT, YH, LZ and ZRT; funding acquisition, PC, ST, MM, LR and ZRT. All authors have read and agreed to the published version of the manuscript.

Funding

This work was partially supported by the NSF (Grant #2230853) and NIST (Grant #70NANB22H010) of the USA.

Acknowledgments

The team would like to thank Paula Prescott and Connie Dixon for ordering lab supplies and managing financial reimbursement. The team also would like to thank Kz Shein, Zay Lynn, and David N. Parette for their technical support.

Conflict of interest

The authors declare no conflict of interest. The funders had no role in the design of the study; in the collection, analyses, or interpretation of data; in the writing of the manuscript, or in the decision to publish the results.

References

1. Benedini L, Laiuppa J, Santillán G, et al. Antibacterial alginate/nano-hydroxyapatite composites for bone tissue engineering: Assessment of their bioactivity, biocompatibility, and antibacterial activity. *Materials Science and Engineering: C* 2020; 115: 111101. doi: 10.1016/j.msec.2020.111101
2. Min Q, Liu J, Zhang Y, et al. Dual network hydrogels incorporated with bone morphogenic protein-7-loaded hyaluronic acid complex nanoparticles for inducing chondrogenic differentiation of synovium-derived mesenchymal stem cells. *Pharmaceutics* 2020; 12(7): 613. doi: 10.3390/pharmaceutics12070613
3. Nie L, Deng Y, Li P, et al. Hydroxyethyl chitosan-reinforced polyvinyl alcohol/biphasic calcium phosphate hydrogels for bone regeneration. *ACS Omega* 2020; 5(19): 10948–10957. doi: 10.1021/acsomega.0c00727
4. Oudadesse H, Najem S, Mosbahi S, et al. Development of hybrid scaffold: Bioactive glass nanoparticles/chitosan for tissue engineering applications. *Journal of Biomedical Materials Research Part A* 2020; 109(5): 590–599. doi: 10.1002/jbm.a.37043
5. Maji K, Dasgupta S, Bhaskar R, et al. Photo-crosslinked alginate nano-hydroxyapatite paste for bone tissue engineering. *Biomedical Materials* 2020; 15(5): 055019. doi: 10.1088/1748-605x/ab9551
6. Wu T, Li B, Wang W, et al. Strontium-substituted hydroxyapatite grown on graphene oxide nanosheet-reinforced chitosan scaffold to promote bone regeneration. *Biomaterials Science* 2020; 8(16): 4603–4615. doi: 10.1039/d0bm00523a
7. Zhang B, Li J, He L, et al. Bio-surface coated titanium scaffolds with cancellous bone-like biomimetic structure for enhanced bone tissue regeneration. *Acta Biomaterialia* 2020; 114: 431–448. doi: 10.1016/j.actbio.2020.07.024
8. Yang L, Gao C, Wei D, et al. Nanotechnology for treating osteoporotic vertebral fractures. *International Journal of Nanomedicine* 2015; 10: 5139–5157. doi: 10.2147/ijn.s85037
9. Saravanan S, Vimalraj S, Anuradha D. Chitosan based thermoresponsive hydrogel containing graphene oxide for bone tissue repair. *Biomedicine & Pharmacotherapy* 2018; 107: 908–917. doi: 10.1016/j.biopha.2018.08.072
10. Mohammadi M, Mousavi Shaegh SA, Alibolandi M, et al. Micro and nanotechnologies for bone regeneration: Recent advances and emerging designs. *Journal of Controlled Release* 2018; 274: 35–55. doi: 10.1016/j.jconrel.2018.01.032
11. Aldaadaa A, Al Qaysi M, Georgiou G, et al. Physical properties and biocompatibility effects of doping SiO₂ and TiO₂ into phosphate-based glass for bone tissue engineering. *Journal of Biomaterials Applications* 2018; 33(2): 271–280. doi: 10.1177/0885328218788832
12. Hashemi A, Ezati M, Mohammadnejad J, et al. Chitosan coating of TiO₂ nanotube arrays for improved metformin release and osteoblast differentiation. *International Journal of Nanomedicine* 2020; 15: 4471–4481. doi: 10.2147/ijn.s248927
13. Liang F, Zhou L, Wang K. Apatite formation on porous titanium by alkali and heat-treatment. *Surface and Coatings Technology* 2003; 165(2): 133–139. doi: 10.1016/s0257-8972(02)00735-1
14. Frandsen CJ, Brammer KS, Noh K, et al. Tantalum coating on TiO₂ nanotubes induces superior rate of matrix mineralization and osteofunctionality in human osteoblasts. *Materials Science and Engineering: C* 2014; 37: 332–341. doi: 10.1016/j.msec.2014.01.014
15. Dong W, Cogbill A, Zhang T, et al. Multifunctional, catalytic nanowire membranes and the membrane-based 3D devices. *The Journal of Physical Chemistry B* 2006; 110(34): 16819–16822. doi: 10.1021/jp0637633
16. Dong W, Zhang T, Epstein J, et al. Multifunctional nanowire bioscaffolds on titanium. *Chemistry of Materials* 2007; 19(18): 4454–4459. doi: 10.1021/cm070845a
17. Hwang C, Park S, Kang IG, et al. Tantalum-coated polylactic acid fibrous membranes for guided bone regeneration. *Materials Science and Engineering: C* 2020; 115: 111112. doi: 10.1016/j.msec.2020.111112
18. Marins NH, Lee BEJ, e Silva RM, et al. Niobium pentoxide and hydroxyapatite particle loaded electrospun polycaprolactone/gelatin membranes for bone tissue engineering. *Colloids and Surfaces B: Biointerfaces* 2019; 182: 110386. doi: 10.1016/j.colsurfb.2019.110386
19. Zhang J, Huang D, Liu S, et al. Zirconia toughened hydroxyapatite biocomposite formed by a DLP 3D printing process for potential bone tissue engineering. *Materials Science and Engineering: C* 2019; 105: 110054. doi: 10.1016/j.msec.2019.110054
20. Inui T, Haneda S, Sasaki M, et al. Enhanced chondrogenic differentiation of equine bone marrow-derived mesenchymal stem cells in zirconia microwell substrata. *Research in Veterinary Science* 2019; 125: 345–350. doi: 10.1016/j.rvsc.2019.07.005
21. Cole P, Tian Y, Thornburgh S, et al. Hydrothermal synthesis of valve metal Zr-doped titanate nanofibers for bone

- tissue engineering. *Nano and Medical Materials* 2023; 3(2): 249. doi: 10.59400/nmm.v3i2.249
22. Xiao Y, Tian Y, Zhan Y, Zhu J. Degradation of organic pollutants in flocculated liquid digestate using photocatalytic titanate nanofibers: Mechanism and response surface optimization. *Frontiers of Agricultural Science and Engineering* 2023. doi: 10.15302/j-fase-2023503
 23. Shannon RD. Revised effective ionic radii and systematic studies of interatomic distances in halides and chalcogenides. *Acta Crystallographica Section A* 1976; 32(5): 751–767. doi: 10.1107/s0567739476001551
 24. Yuan ZY, Zhang XB, Su BL. Moderate hydrothermal synthesis of potassium titanate nanowires. *Applied Physics A* 2004; 78(7): 1063–1066. doi: 10.1007/s00339-003-2165-x
 25. Wu Z, Yoshimura M. The formation of pyrochlore potassium tantalate thin films by soft solution processing. *Thin Solid Films* 2000; 375(1–2): 46–50. doi: 10.1016/s0040-6090(00)01178-0
 26. Alizadeh A, Moztaarzadeh F, Ostad SN, et al. Synthesis of calcium phosphate-zirconia scaffold and human endometrial adult stem cells for bone tissue engineering. *Artificial Cells, Nanomedicine, and Biotechnology* 2014; 44(1): 66–73. doi: 10.3109/21691401.2014.909825
 27. Jin S, Yu J, Zheng Y, et al. Preparation and characterization of electrospun PAN/PSA carbonized nanofibers: Experiment and simulation study. *Nanomaterials* 2018; 8(10): 821. doi: 10.3390/nano8100821
 28. Wang X, Liu SJ, Qi YM, et al. Behavior of potassium titanate whisker in simulated body fluid. *Materials Letters* 2014; 135: 139–142. doi: 10.1016/j.matlet.2014.07.145
 29. Kokubo T, Yamaguchi S. Novel bioactive titanate layers formed on Ti metal and its alloys by chemical treatments. *Materials* 2009; 3(1): 48–63. doi: 10.3390/ma3010048